International Journal of Modern Manufacturing Technologies
ISSN 2067–3604, Vol. XVI, No. 3 / 2024
https://doi.org/ 10.54684/ijmmt.2024.16.3.21

MECHANICAL PROPERTIES OF 3D PRINTED PLA/FISH SCALES HYDROXYAPATITE COMPOSITE FOR BIOMEDICAL APPLICATIONS

Che Nor Aiza Jaafar[1], Muhammad Izham Ismail[1], Ismail Zainol[2], Mani Raj Narthan[1]

[1]Department of Mechanical and Manufacturing Engineering, Faculty of Engineering, University Putra Malaysia, 43400 UPM Serdang Selangor Darul Ehsan, Malaysia
[2]Chemistry Department, Faculty of Science and Mathematics, Universiti Pendidikan Sultan Idris, 35900 Tanjong Malim, Perak, Malaysia

Corresponding author: Che Nor Aiza Jaafar, cnaiza@upm.edu.my

Abstract: Researchers around the world are currently still investigating the possibility of using poly(lactic acid) (PLA)/hydroxyapatite (HAp) composite as a biomaterial. However, most of the research published utilized synthetically derived hydroxyapatite (HAp) which is more expensive than natural-based HAp. Hence, this project aims to investigate the reliability in terms of mechanical properties of the PLA/fish scales derived HAp (FsHAp) biocomposite comprised of PLA and FsHAp as a filler at various compositions ranging from 10 to 40 wt%. The PLA/FsHAp composite filaments were developed through melt blending of PLA resin and FsHAp powder by a twin screw extruder. The test specimen was prepared by 3D printing of composite filament using a Creality CR 6-SE 3D printer. However, the composite with filler content above 30 % failed to convert into filament due to the inherent brittleness of PLA/FsHAp composite. Hence, the mechanical properties were only analyzed for PLA, 10 and 20 wt% of PLA/FsHAp composites. The 20 wt% FsHAp filler content displayed higher tensile and flexural properties than 10 wt% despite the reduction in impact properties. In this study, the 20 wt% also indicates a better dispersion and reinforcing effect of the FsHAp filler on the PLA matrix. Overall results concluded that the addition of natural FsHAp fillers has a direct influence on the mechanical properties of PLA/FsHAp composite with the support of FTIR and SEM analysis. The composite has the potential to be used in the fabrication of medical device implants using 3D printing technique

Keywords: poly(lactic acid) (PLA), fish scales hydroxyapatite (FsHAp), PLA/FsHAp composite, 3D printing.

1. INTRODUCTION

Traditional treatment for bone defects usually requires the grafting of bone which have many limitations that could contribute to adverse effects on the addressing the risk of infection and bone tissue healing process. For example, when a larger bone defect area fails to be stabilized by a fixed implant from a bone graft, dead cavities will develop as a result of inadequate bone marrow occupancy [1]. At present, the potential of 3D printing in medical applications is paving the innovative growth, including the regeneration of damaged tissues and organs [2]. As proof, 3D printing is used to stimulate regeneration to conserve existing bone and encourage osteogenesis to achieve comprehensive bone healing and restore normal anatomical structure and function around the craniofacial region [3]. Hence, 3D printing is a definite solution to address complex bone defect challenges that were experienced by both humans and animals. Fundamentally, bone tissue engineering involves the development of scaffolds as a treatment. A scaffold is designed and developed as an approach to transporting new cells to a specific area within the human or animal body and acts as a framework for the growth of newly forming tissue [4]. With the presence of 3D printing technology, the development of medical scaffolds has become more straightforward and advanced over time. Soleymani & Naghib [5] reported that medical scaffolds were developed through various conventional methods such as gas foaming, solvent-casting particulate-leaching, freeze-drying, and solution casting in the past. However, this traditional technique possesses several restrictions such as inaccurate pore size, and pore geometry, and failed to achieve adequate interconnectivity and sufficient mechanical strength. To counter this problem, 3D printing technology has proven its potential to generate extraordinary levels of accuracy and precision in the development process of medical scaffolds [5].

In general, human bone in general is made up of two components which are inorganic components (HAp) and an organic matrix such as collagen. In tissue engineering, HAp has been utilized as a bone substitute material. However, pure HAp is typically fragile and must be paired with a suitable polymer to decrease the brittleness of Hap [6]. In addition, past studies have indicated that PLA is currently one of the highest potential polymers with a sustainable eco-friendly characteristic which makes it suitable to be deployed as the 3D printed scaffold material in the field of bone tissue engineering. Although PLA plays a crucial role in implementing various strategies related to tissue engineering and regenerative medicinal treatment, PLA contains several mechanical constraints in terms of its engineering application. This is due to the low toughness characteristic which makes it a relatively brittle material as it exhibits less than 10% elongation before it [7]. Donate et al. [8] suggests that bioceramics should be utilize as additives to improve and optimize the biological and mechanical properties of the PLA-based scaffolds and at the same time increasing the potential for altering its biodegradation profile and the fabrication rate. Hence, the weakness of PLA can be overcome by reinforcing it with bioceramic HAp to enhance its mechanical properties. Today, commercialized HAp is mostly obtained through various chemical processes such as chemical precipitation [9]. Venkatraman et al. [10] criticized that the production of synthetic HAp is quite complex and costly in contrast to natural HAp which is more economical and has a straightforward synthesis process. Therefore, this project will emphasize the use of natural HAp made from fish scales as the additive to PLA polymer for development of medical scaffold for biomedical applications using 3D printing technology. By using natural HAp made from fish scales (FsHAp), the environmental pollution could be reduced significantly as fish scales if left unintended will cause a harmful effect in open space mainly in coastal areas [11].

2. MATERIALS AND METHODS

2.1. Materials

In this project, two main materials were utilized which are poly(lactic acid) (PLA) and natural hydroxyapatite which is extracted from Tilapia fish scales (FsHAp). The PLA polymer resin (Luminy LX575) was acquired from Total Corbion, Thailand while the FsHAp powder used in the project was processed by utilizing the ashes of fish scales derived from Tilapia fish *(Oreochromis niloticus*). For synthesis of FsHAp powder, a wet method ball milling was utilized to crush the ashes of fish scales into finer size. The process was carried out for at least 72 hours continuously. Then, the slurry FsHAp liquid was oven dried at 80 to 100 °C overnight or until it is fully dried. The dried solid of FsHAp was then blended to crush the solid chunks into powder. Fig. 1 displays the raw material utilized for this project.

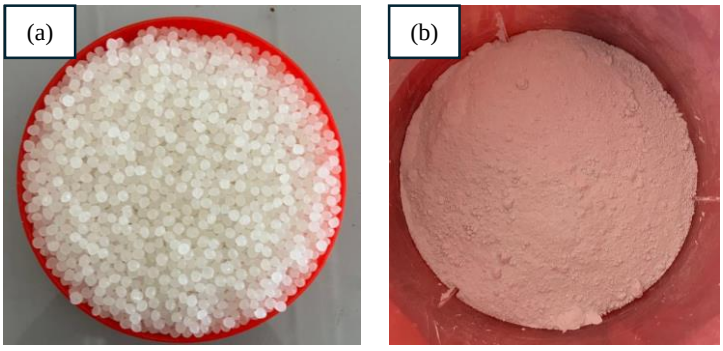

Fig. 1. The raw materials used: (a) PLA resins and (b) FsHAp powder

2.2. Fabrication of PLA/FsHAp Composite Filaments Feedstock for 3D Printer

The fabrication of the PLA/FsHAp composite emphasized the development of polymer composites in the form of 3D printing filament feedstock. The fabrication process of the PLA/FsHAp composite filaments was composed of 4 crucial steps. The first step was to dry mix both PLA and FsHAp powder based on the predetermined compositions as shown in Table 1.

Table 1. The formulation of the PLA/FsHAp composite samples

Sample	PLA/ 0FsHAp	PLA/ 10FsHAp	PLA/ 20FsHAp	PLA/ 30FsHAp	PLA/ 40FsHAp
PLA (wt%)	100	90	80	70	60
FsHAp (wt%)	100	10	20	30	40

The second step was the melt blending of the batch formulation with the help of twin screw extruder to compound both PLA and FsHAp powder together. The third step was the grinding process of the PLA/FsHAp composites filament into pallet forms. As the final step, the pallets of the PLA/FsHAp composites were hot extruded to obtain the filaments for 3D printer using wood filament extruder machine which was manufactured by Dongguan Songhu Plastic Machinery Co., Ltd to produce filaments with a consistent diameter of 1.75mm which is a standard diameter for fused deposition modelling (FDM) 3D printing. In this process also, the filaments for the PLA/30FsHAp and PLA/40FsHAp compositions were unable to be produced due to the significant brittleness of the polymer composite. This constraint was manifest during the process, wherein both compositions consistently failed to be manually drawn due to its breaking at multiple points within the water bath section. Only 10 wt% and 20 wt% of filler compositions for the PLA/FsHAp composites were able to produce. Fig. 2 illustrates the final form of the PLA/FsHAp composite filaments obtained from the fabrication process.

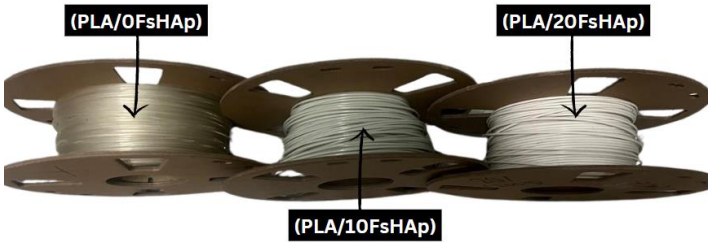

Fig. 2. The spool of filaments made from PLA and FsHAp powder at different fillers content

2.3. 3D Printing Process of the PLA/FsHAp Composite Filaments

The testing specimens of this study were obtained by using the method of fused deposition modelling (FDM) 3D printing where the PLA/FsHAp composite filaments are extruded at its molten state through a nozzle which moves based on the instruction provided in the form of G-codes from the slicer. In this process, SolidWorks was utilized to create the 3D model design of the required specimens according to ASTM standards. Meanwhile, the 3D printer used for the fabrication of the specimens was Creality CR-6 SE and the slicer used was Ultimaker Cura 5.5.0 software with the infill pattern of lines and density of 99.9%. In this project, 3 types of specimens were 3D printed based on the required design for the intended mechanical testing which are tensile test, impact test and flexural test. Table 2 displays the crucial parameters used during the FDM 3D printing of the PLA/FsHAp composites while Fig.3 displays the 3D printed specimen for the mechanical testing for this project with the bottom position indicates pure PLA, middle position indicates 10 wt% of FsHAp filler content and the upper position indicates the 20 wt% of FsHAp filler content.

Table 2. The 3D printing parameters used for this project

Settings	Specification
Nozzle Diameter	0.4 mm
Printing Temperature	220 °C
Build Plate Temperature	70 °C
Print Speed	100 mm/s
Fan Speed	100 %
Support	No
Build Plate Adhesion Type	Skirt

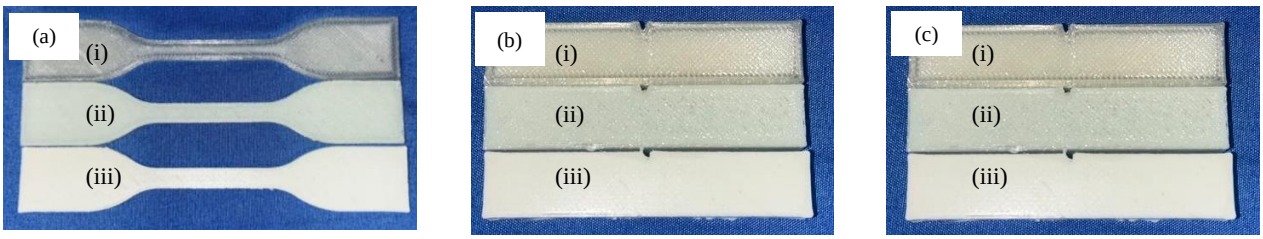

Fig.3. The 3D printed specimen for (a) tensile testing, (b) impact testing and (c) flexural testing and (i), (ii) and (iii) for PLA, PLA/10FsHAp and PLA/20FSHAp respectively

2.3. Fourier Transforms Infrared Spectroscopy (FTIR) Analysis

The FTIR analysis was carried out to identify the chemical properties of functional groups of the prepared samples. In this analysis, the specimen of the 3D printed PLA/FsHAp composites and pure PLA were scraped into powders and using ATR accessories, the samples were scanned in the range from 4000 cm^{-1} to 525 cm^{-1} using Fourier transform infrared (FTIR) spectrometer (Thermo Scientific Nicolet iS10).

2.4. Mechanical Properties Analysis

The mechanical properties analysis of the 3D printed PLA/FsHAp composites was divided into 3 parts which are impact testing, tensile testing and flexural testing. All the testing were carried out based on the ASTM standards methods.

2.4.1. Tensile Testing

The tensile test was carried out based on ASTM D638. The tensile strength, Young's modulus and elongation at break of the 3D printed specimens were recorded using a universal testing machine (INSTRON, Model 3365).

2.4.2. Impact Testing

The impact test was carried out by utilizing Izod impact test through Ray-Ran Advance Universal Pendulum Impact Tester machine according to ASTM D256. The test specimens were prepared using the 3D printing method. This assessment is important to determine the 3D-printed specimens' ability to withstand sudden impacts and fractures.

2.4.3. Flexural Testing

The flexural test was carried out using ASTM D790. The purpose of the flexural test is to evaluate the flexural strength and flexural modulus of the 3D-printed PLA/FsHAp composite specimens. Flexural test which was also known as the three-point bending test, was carried out by using a universal testing machine (INSTRON, Model 3365).

2.3. Morphology Analysis

The SEM analysis was carried out using JSM6400 Scanning Electron Microscope. The purpose of this analysis was to evaluate the microstructure of the 3D printed specimen and to study the effects of the FsHAp filler composition on the microstructure of the 3D printed PLA/FsHAp composite. In this analysis, the fractured surface of the 3D printed PLA/FsHAp specimens resulting from the impact test was coated with gold to improve the quality of the image produced and to prevent electrostatic charging.

3. RESULTS AND DISCUSSION

3.1. FTIR Analysis

Fig. 4 displays the overlaid FTIR spectra of virgin PLA resin, 3D printed PLA, PLA/0FsHAp, PLA/10FsHAp and PLA/20FsHAp. The FTIR spectra of virgin PLA (Fig. 4a) and 3D printed PLA (Fig. 4b) were identified to be very similar which indicated no big changes in the chemical structure after a few processing steps to produce 3D printed specimen. The prominent peak for PLA appears at 2922 and 2945 cm-^{1} for CH_3 groups. Despite the slight differences in the wave number of the CH_3 stretching peak, the ester groups of PLA could be identified in both FTIR spectra of PLA resins at 1747, 1180, 1083, and 1043 cm^{-1} while at 1746, 1180, 1079 and 1043 cm^{-1} for 3D printed PLA specimen [12]. Furthermore, the bands at 1747 cm^{-1} for Figure 4.7 (a) and 1746 cm^{-1} indicates the vibrations of the functional group of C=O stretching meanwhile the peaks at 1267 cm^{-1} of PLA resins and 1266.58 cm-1 of 3D printed PLA specimen correspond to the C-H bending. In addition, Fig. 4(a) and (b) both highlighted the bending of OH group at the bands of 956 and 956 cm^{-1} respectively [12].

Fig. 4(c) and (d) display the FTIR spectra of 3D printed PLA/FsHAp composites of 10 and 20 wt% of FsHAp filler composition. From the chemical bonding interaction of PLA matrix and FsHAp polymer matrix, a new stretching of functional group C=O was developed at 1746 and 1747 cm^{-1} wave number respectively. In addition, the vibrations of functional group PO_4^{-3} were also identified for both spectrum of Fig. 4 (c) and (d) at the wave number of 1081 and 1081 cm^{-1} respectively due to the incorporation of FsHAp fillers. According to Tazibt et al. [13], the intensity of absorption band correlates with the PO_4^{-3} vibration in the FsHAp powder; hence, the intensity increases as the FsHAp filler content increases. Moreover, it was observed that both PLA/FsHAp composites formed extra peaks at the wave numbers of 601 and 570 cm^{-1} for 10 wt% of FsHAp filler composition while 600 and 568 cm^{-1} for 20 wt% of FsHAp filler composition. The formation of the extra peaks could be due to further

unidentified interactions between the FsHAp filler and PLA polymers. Fig. 4 (e) showcases the FTIR spectrum of the processed FsHAp powder. There are several functional groups that could be identified from the peaks formed showing the characteristics of a ceramic which consist of phosphate (PO_4^{-3}), hydroxyl (OH^-) and carbonate (CO_3^{-2}). The vibration of phosphate group was identified at the 2 strong peaks of 1012 and 568 cm^{-1} respectively. In addition, the hydroxyl group was identified at the peak of 629.39 cm^{-1} while the carbonate group was identified at the peak of 961 cm^{-1}.

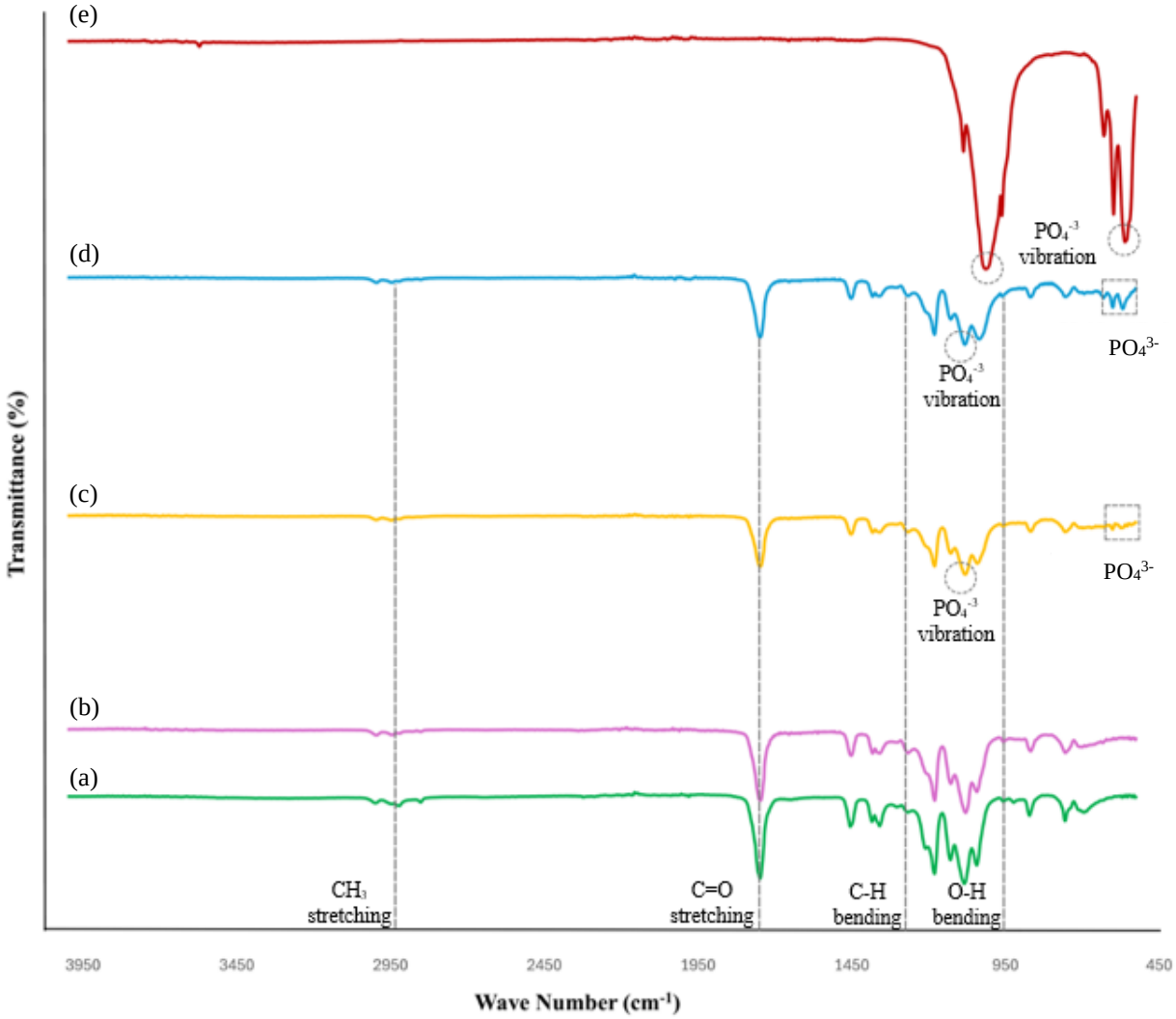

Fig. 4: The FTIR spectra of (a) PLA resins, (b) PLA/0FsHAp, (c) PLA/10FsHAp, (d) PLA/20FsHAp and (e) FsHAp powder

3.2. Mechanical Propertie Analysis

The mechanical properties of the PLA/FsHAp 3D Printed composite was assessed in terms of tensile properties, impact properties and flexural properties. The test was conducted to investigate the influence of FsHAp fillers wt% to the overall mechanical properties of the PLA/FsHAp 3D Printed composites. However, the subsequence section could only discuss the influence of FsHAp fillers wt% only up to 20 wt% due to the failed acquisition of the PLA/FsHAp composite filament for the 30 wt% and 40 wt% of FsHAp filler content during the filament fabrication process which could be attributed to the significant brittleness of these two compositions.

3.2.1. Tensile Properties Analysis

The addition of FsHAp as filler to PLA polymers have a significant influence on the tensile properties of the PLA/FsHAp composites regardless of the fabrication method. Fig. 5 highlights the influence of FsHAp fillers wt% to the tensile strength of the PLA/FsHAp composites.

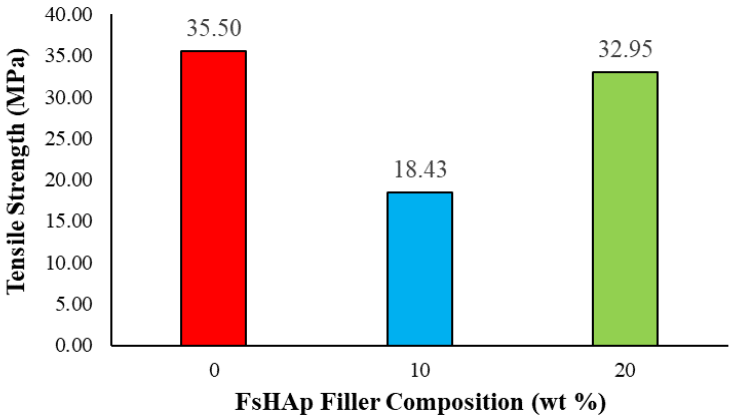

Fig. 5. The tensile strength for the different filler compositions of the 3D printed PLA/FsHAp composites

An interesting pattern could be observed as the addition of FsHAp fillers both 10 wt% and 20% provide a different response in terms of the tensile strength of the PLA/FsHAp 3D printed composites. At 0 wt% of 3D printed PLA/0FsHAp or pure PLA, the tensile strength obtained was 35.50 MPa which is significantly lower than the standard tensile strength of pure PLA (50 MPa to 60 MPa). The results of tensile strength obtained for 3D printed specimens were lower than standard PLA probably attributed to the formation of defects that occur during the FDM 3D printing process. Theoretically, the fused deposition modeling (FDM) 3D printing process should produce precisely aligned geometries with strong interlayer of adhesion; however, the heating and cooling of the thermoplastic causes expansion, compression, and sometimes changes in crystallinity leading to high internal stresses, can result in defect formation at both macro and micro levels in practice. These defects can arise due to the inherent material characteristics (such as composition) or suboptimal printing parameters [14]. In addition, PLA is also known for its hydrophobicity. It was suspected that during the 3D printing process, the surrounding environment caused the PLA filament to degrade in general due to the presence of moisture in the environment. According to Nadzi & Karlsson [15], PLA is sensitive to moisture, which can lead to hydrolysis, a chemical reaction that breaks down the polymer chain in general. This reaction decreases the molecular weight of PLA and is regarded as a preliminary step before biodegradation. Zhang et al. [16] reported that extended exposure to moisture will cause hydrolysis of PLA at a higher rate which reduces tensile strength and Young's modulus of PLA.

Based on the results obtained also, the incorporation of 10 wt% of FsHAp fillers to the PLA polymer has lower tensile strength compared to pure PLA and 20 wt% of FsHAp fillers composition. This is because the tensile strength of PLA/10FsHAp was 18.43 MPa which is significantly lower than PLA/20FsHAp or pure PLA of 35.5 MPa. This was suspected to be caused by the lack of reinforcement effect of FsHAp which is not enough to provide substantial support in terms of tensile strength in the PLA/10FsHAp structure. Despite this, the incorporation of 20 wt% of FsHAP filler to PLA polymer of the 3D printed PLA/20FsHAp has shown a substantial magnitude of tensile strength of 32.95 MPa which was quite close to the tensile strength of pure PLA. Due to this, it can be assumed that the 20 wt% have a better reinforcing effect and dispersion in the PLA polymer matrix compared to 10 wt% of FsHAp filler content. Hence, this explained the pattern formed as the tensile strength decreases at 10 wt% and increases at 20 wt% of FsHAp filler composition.

Literature has agreed that the mechanical properties of PLA/Hap composites are heavily dependent on the dispersion of the HAp in the PLA matrix [17]. However, there are various factors that could affect the mechanical properties of the PLA/FsHAp composites. According to Custodio et.al [12], the reduction in tensile strength of PLA/HAp composite was heavily associated with the poor dispersion, agglomeration and the formation of macro voids among adjacent filament beads despite the reinforcing effect that HAp had. Through the effect of mechanical interlocking, HAp could potentially serve as nucleation sites, facilitating the entanglement of PLA molecule chains.

Fig. 5 represents the Young's modulus exhibited by the PLA/FsHAp 3D printed composites from 0 wt% to 20 wt% of FsHAp filler content. Based on the results obtained, the PLA/0FsHAp or pure PLA displayed a Young's modulus of 1507 MPa which was significantly lower than the theoretical Young's modulus for the Luminy® LX575 PLA of 3500 MPa. For the analysis of Young's modulus of the tensile properties, an interesting pattern was obtained as the wt% of the FsHAp filler increases from 10 wt% to 20 wt%. Through the incorporation of FsHAp fillers up to 10 wt%, the Young's modulus drastically decreases to 963.56 MPa compared to the Young's modulus of pure PLA.

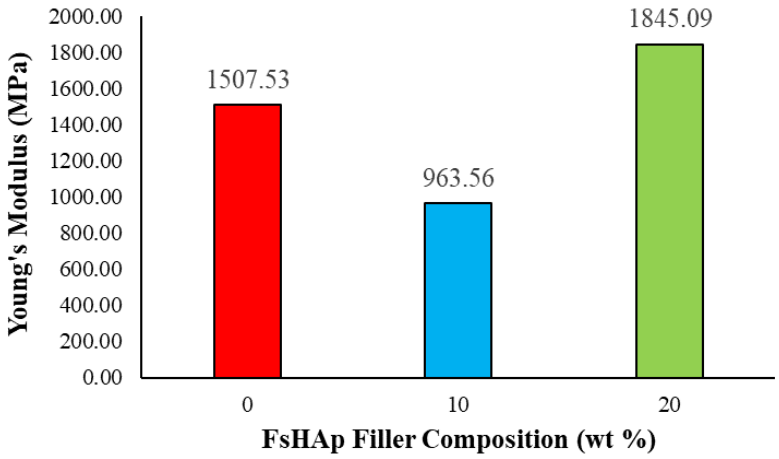

Fig. 5. The Young's modulus for the different filler composition of the 3D printed PLA/FsHAp composites

However, a different result was shown when the incorporation of 20 wt% FsHAp fillers was utilized. The Young's modulus of the PLA/20FsHAp 3D printed composites increased to 1845 MPa which was significantly higher than Young's modulus of pure PLA. According to Dubinenko et al. [18], a notable increment of Young's modulus is commonly associated with the uniform distribution of efficiently dispersed HAp powder together with strong bonding between the HAp filler and PLA matrix. Hence, this indicates that the PLA/10FsHAp exhibits poor dispersion of FsHAp fillers to the PLA polymer matrix while the PLA/20FsHAp exhibits a better quality of dispersion which heavily influences the Young's modulus obtained.

In addition to tensile strength and Young's modulus, the analysis for elongation at break was also carried out for the characterization of tensile properties. Fig. 6 portrayed the percentage of elongation at break for the PLA/FsHAp 3D printed composites with different compositions of FsHAp fillers from 10 wt% to 20 wt%. A similar trend was observed to occur for the analysis of elongation at break compared to the analysis of Young's modulus. The elongation of break for 3D printed PLA/0FsHAp or pure PLA was calculated to be at 2.7%. The addition of fillers with 10 wt% compositions for the 3D printed PLA/10FsHAp lowered the elongation at break value to 2.61% which is quite lower than PLA/0FsHAp. As a flexible polymer in nature, PLA exhibits a higher value of elongation at break compared to the brittle nature of ceramics in theory [19]. This explains the significant reduction in the breaking elongation for the 10 wt% of FsHAp fillers composition.

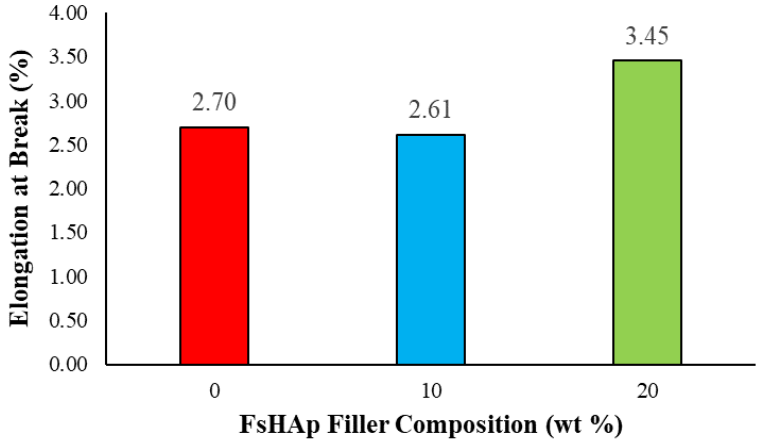

Fig. 6. The elongation at break for the different filler composition of the 3D printed PLA/FsHAp composites

However, the elongation at break for the 20 wt% FsHAp filler composition of the 3D printed PLA/20FsHAp shown a significant increase to 3.45 % which was higher than the elongation at break of the pure PLA. These results could probably be attributed to the quality of FsHAp fillers dispersion to the matrix of the PLA polymer. In this case, the 20 wt% has successfully dispersed homogenously compared to 10 wt% which provides a better support in terms of interfacial adhesion.

3.2.2. Impact Properties Analysis

Impact property was essential part of the characterization of the mechanical properties for the 3D printed PLA/FsHAp composites. Fig. 7 displays the impact strength of the 3D printed PLA/FsHAp composites with different FsHAp filler content ranging from 0 wt% to 20 wt%.

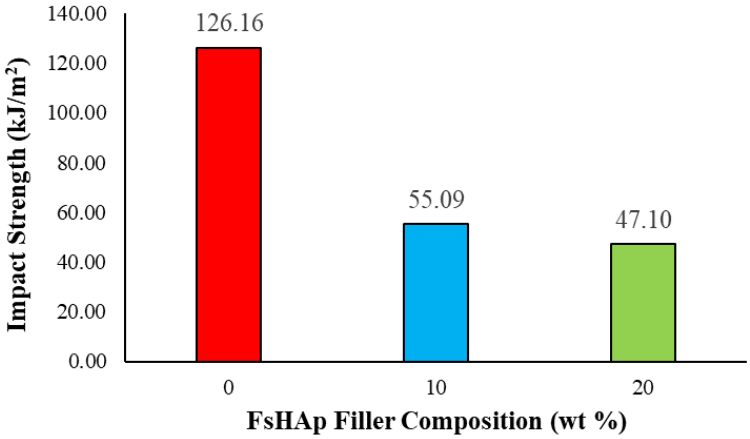

Fig. 7. The impact strength for the different filler compositions of the 3D printed PLA/FsHAp composites

As seen in Fig. 7, it can be described as the addition of FsHAp fillers to PLA polymer reduces the impact strength of the 3D printed PLA/FsHAp composites. This is due to 3D printed PLA/0FsHAp or pure PLA displaying the highest value of impact strength of 126.16 kJ/m2 for all three compositions. The 3D printed PLA/10FsHAp exhibited an impact strength of 55.09 kJ/m2 which was significantly lower than pure PLA while the 3D printed PLA/20FsHAp displayed the weakest impact strength of 47.10 kJ/m2 among all compositions. The result obtained from the impact test was aligned with the research study by Tazibt et al. [13] which stated that the impact strength decreases as the HAp filler content increases. Tazibt et al. [13] also reported that the agglomeration of HAp particles in the PLA matrix decreases the contact area, introduces physical defects, and restricts the movement and deformation of the PLA polymer chains. All these factors contribute to the reduction not only impact properties but also tensile properties in terms of tensile strength and elongation at the break of the PLA/HAp composite. Therefore, this situation will be further confirmed through SEM analysis which will be discussed in the morphological analysis subsection.

3.2.3. Flexural Properties Analysis

In addition to tensile and impact properties, flexural properties is also an essential factor in determining the mechanical properties of the 3D printed PLA/FsHAp composites. The flexural properties of the 3D printed PLA/FsHAp composites could be described through two aspects, namely: flexural strength and flexural modulus. Fig. 8 presents the flexural strength for the 3D printed PLA/FsHAp composite with various FsHAp filler content ranging from 0 wt% to 20 wt%. From Fig. 8, the 3D printed PLA/0FsHAp exhibited the highest flexural strength of 54.37 MPa. The incorporation of FsHAp fillers up to 10 wt% to the PLA polymer have shown to decrease the magnitude of the flexural strength to 33.67 MPa. However, at 20 wt% of FsHAp filler, the 3D printed PLA/FsHAp displayed an increment of flexural strength to 39.12 MPa which was slightly higher than the flexural strength of the 3D printed PLA/10FsHAp but still significantly lower than the flexural strength of the 3D pure PLA. The result obtained from the flexural test of Ferri et al. [19] which the reported that the flexural strength decreases as the FsHAp filler content increases. Moreover, the dispersal of FsHAp particles decreases at higher FsHAp filler content in the PLA/FsHAp composite because of higher viscosity in properties. However, it is suspected that the 3D printed PLA/10FsHAp composite has an extremely poor dispersion of FsHAp filler to the PLA matrix as the flexural strength was supposed to be higher than the 3D printed PLA/20FsHAp composite. This causes a severe limitation to the flexural properties of the 3D printed PLA/10FsHAp composite.

Furthermore, Fig. 9 displays the flexural modulus for the 3D printed PLA/FsHAp composite with various FsHAp filler content ranging from 0 wt% to 20 wt%. Compared to the result obtained for the flexural strength, the result of the flexural modulus exhibits a similar pattern in general. The 3D printed PLA/0FsHAp or pure PLA displayed the highest flexural modulus of 2335.59 MPa among all composition. The flexural modulus of the 3D printed PLA/10FsHAp decreased to 1944.07 MPa which is lower than the flexural modulus exhibited by the 3D printed of pure PLA. Despite the decrement in flexural modulus through the incorporation of FsHAp fillers, the 3D printed PLA/20FsHAp with 20 wt% FsHAp filler composition showed a better result in term of flexural modulus of 2005.19 which was slightly higher than the flexural modulus of the 3D printed 10 wt% FsHAp filler composition.

From this trend, it can be summarized that the influence of FsHAp filler's dispersion have a significant amount of influence on the flexural properties of the PLA/FsHAp composite. This is contradicted with the result obtained by Ferri et al. [19] which reported the flexural modulus increases as the HAp filler content increases. This situation could be attributed to the presence of defects and the possibility of deformation that occurs to the PLA/FsHAp composite during the FDM 3D printing process and the filament fabrication process as discussed earlier.

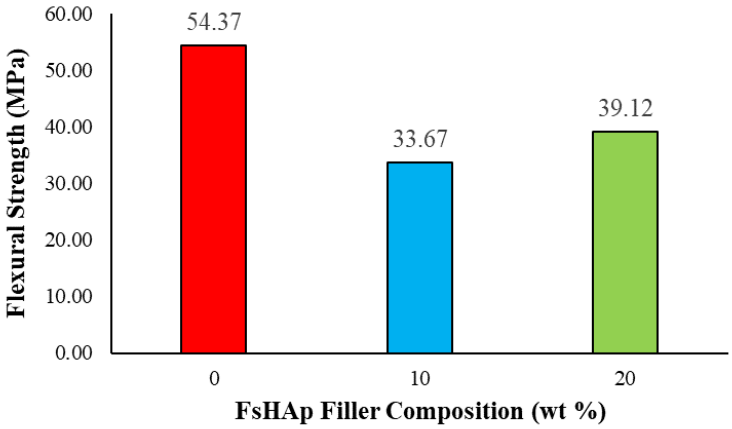

Fig. 8. The flexural strength for the different filler composition of the 3D printed PLA/FsHAp composites

3.3. Morphology Analysis

To further justify the result obtained from the mechanical testing, scanning electron microscopy (SEM) was utilized to investigate the microstructure of the 3D printed PLA/FsHAp with different FsHAp filler content ranging from 0 wt% to 20 wt%. Fig. 10 illustrates the microstructure obtained from the fractured surface of 3D printed samples of impact tests at 2500 x magnification.

It was also observed that the incorporation of FsHAp filler to the matrix of PLA polymer has a significant influence on the surface texture of the microstructure of the 3D printed PLA/FsHAp composite. Fig. 9 (a) of pure PLA illustrates a smoother surface compared to the rougher surface displayed in Fig. 9(b) and (c) of 3D printed the PLA/FsHAp composites. According to Peremel et.al [20], a rougher surface of PLA/FsHAp composites tend to be find at higher FsHAp filler contents.

Fig. 9 (a) shows the morphology of the fractured surface of the 3D printed impact specimen of PLA/0FsHAp or pure PLA. It was observed that there was a presence of voids and surface cracks of various sizes on the smooth surface of the pure PLA. It is suspected that these voids and surface cracks were results from the defect during the filaments fabrication process of 3D printing. This situation could be further attributed to the lack of drying time to remove the moisture from the PLA pallets. Hence, the formation of these defects leads to a significant reduction in the mechanical properties of the 3D printed PLA/0FsHAp samples. This explained the values obtained for the analysis mechanical testing conducted for the 3D printed of PLA/0FsHAp which are not within the standard range of the mechanical properties of general PLA.

Fig. 9 (b) and (c) both display the morphology of the fractured surface for the 3D printed PLA/10FsHAp and PLA/20FsHAp impact test specimen respectively. Both Fig. 10 (b) and (c) show that the distribution of spherical shape of the FsHAp filler particle.

According to Ferri et al. [19] for the utilization of spherical shape hydroxyapatite is more advantages as it the particle size to exibit a wider span of coverage. Despite the tendency of uniform dispersion, the possibility of agglomeration also presence due to the spherical shape of the FsHAp filler particles.

According to Baechle-Clayton et al. [21], the lack of uniformity in the composition is a significant factor in the reduction of mechanical properties and leads to stress concentration in specific areas or weak regions of the composite material. It was observed that Fig. 9 (c) of 20 wt% FsHAp filler indicates a finer and more homogenous dispersion of filler particle compared to Fig. 9(b) of 10 wt% of FsHAp filler. However, the agglomeration and the formation of voids for the 10 wt% FsHAp filler was significantly higher than the 20 wt% FsHAp filler. According to Tazibt et al. [13], premature failure of material is caused by the presence of filler aggregates which serves as a stress concentration points within the composite microstructure. Due to this, the mechanical properties of the 3D printed PLA/10FsHAp composite is significantly reduced compared to the 3D printed PLA/20FsHAp composite and pure PLA. For composite materials, the mechanical properties were influenced not solely by the interfacial bonding between matrix and filler, but also by the dispersion of the filler [22].

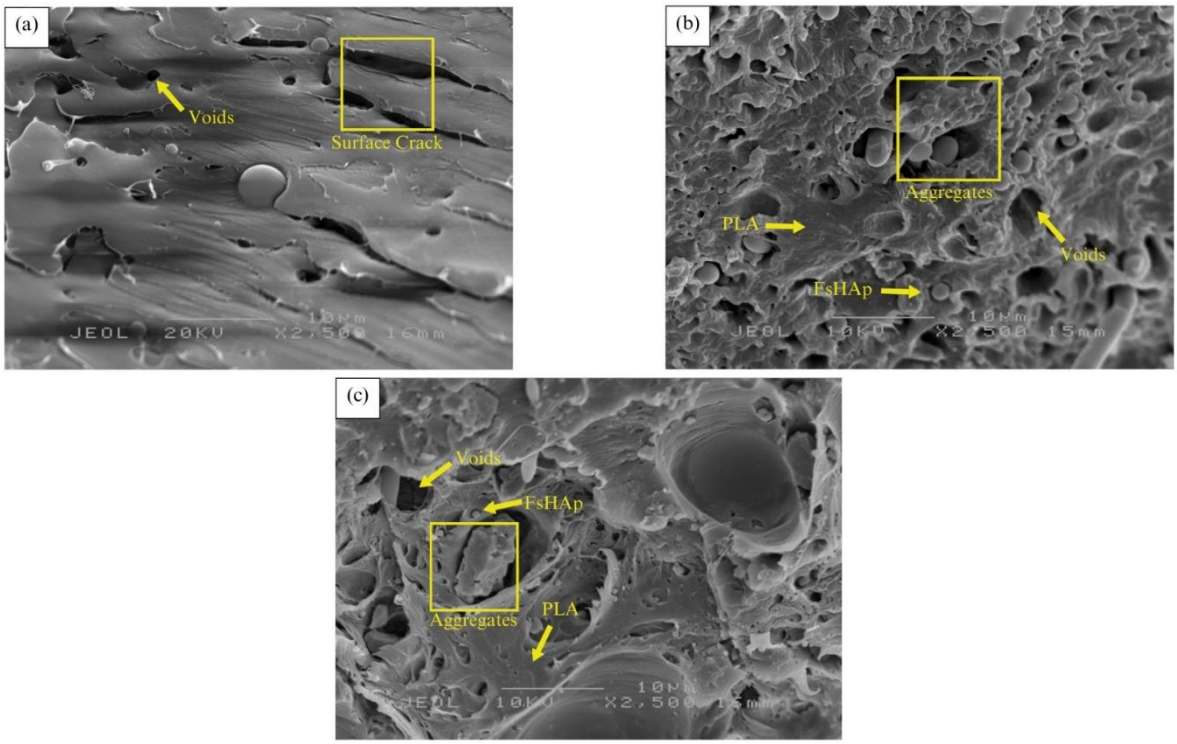

Fig. 9. The microstructure obtained from SEM analysis of the 3D printed of (a) pure PLA, (b) PLA/10FsHAp and (c) PLA/20FsHAp

4. CONCLUSIONS

The incorporation of FsHAp filler to PLA matrix polymer heavily influenced the mechanical properties of the PLA/FsHAp composite in general. From this project, the FTIR analysis and the mechanical properties characterization of the PLA/FsHAp composite reveal significant insights and information into the effects of FsHAp filler on the structure of the PLA/FsHAp composite obtained through FDM 3D printing. The FTIR spectra successfully indicate the presence of functional groups and the interaction between PLA and FsHAp, with observed changes in wave numbers due to filler incorporation. Due to this, the mechanical properties analysis shows that adding FsHAp fillers impacts tensile strength, impact strength, and flexural properties, with variations observed at different FsHAp filler concentrations up to 20 wt%. The 20 wt% FsHAp filler content successfully demonstrates improved dispersion and reinforcing effects compared to 10 wt% filler content; therefore, enhancing certain mechanical properties such as Young's modulus (1845.09 Mpa) and elongation at break (3.45%). However, higher filler at 20 wt% FsHAp filler content also introduces challenges such as reduced impact strength (47.10 kJ/m^2) and potential agglomeration. This finding was supported by SEM analysis which illustrates the influence of FsHAp fillers on microstructure, including surface roughness and void formation. Overall, this study emphasizes the complex relationship between FsHAp filler content, dispersion quality, and mechanical performance in PLA/FsHAp composites fabricated through FDM 3D printing while in search for optimal filler composition for achieving desired properties as a polymer composite intended for biomedical applications.

Funding: This research was supported by the UPM Putra grant under vote number 9683900. We thank Universiti Putra Malaysia for their support during the research.
Conflicts of Interest: There is no conflict of interest.

REFERENCES

1. Chen, J., Zhou, H., Fan, Y., Gao, G., Ying, Y., Li, J. (2023). *3D printing for bone repair: Coupling infection therapy and defect regeneration*. Chemical Engineering Journal, 471, 144537.
2. Pradeep, P., Paul, L. (2022). *Review on novel biomaterials and innovative 3D printing techniques in biomedical applications*. Materials Today: Proceedings, 58, 96–103.
3. Maroulakos, M., Kamperos, G., Tayebi, L., Halazonetis, D., Ren, Y. (2019). *Applications of 3D printing on craniofacial bone repair: A systematic review*. Journal of Dentistry, 80, 1–14.
4. Bozkurt, Y., Karayel, E. (2021). *3D printing technology; methods, biomedical applications, future opportunities and trends*. Journal of Materials Research and Technology/Journal of Materials Research and

Technology, 14, 1430–1450.
5. Soleymani, S., Naghib, S. M. (2023). *3D and 4D printing hydroxyapatite-based scaffolds for bone tissue engineering and regeneration.* Heliyon, 9(9), e19363.
6. Bogala, M. R. (2022). *Three-dimensional (3D) printing of hydroxyapatite-based scaffolds: A review*. Bioprinting, 28, e00244.
7. DeStefano, V., Khan, S., Tabada, A. (2020). *Applications of PLA in modern medicine*. Engineered Regeneration, 1, 76–87.
8. Donate, R., Monzón, M., Alemán-Domínguez, M. E. (2020). *Additive manufacturing of PLA-based scaffolds intended for bone regeneration and strategies to improve their biological properties*. E-Polymers, 20(1), 571–599.
9. Majhooll, N. a. A., Zainol, N. I., Jaafar, N. C. N. A., Mudhafar, N. M., A, N. a. H., Asaad, N. A., Mezaal, N. F. W. (2019). *Preparation of fish scales hydroxyapatite (FSHAP) for potential use as fillers in polymer*. Journal of Chemistry and Chemical Engineering, 13(3).
10. Venkatraman, P., Rajan, R., Sureka, C., Nehru, L. (2023). *Synthesis and fabrication of HAp from fish scale waste to develop bone equivalent phantom*. Nuclear and Particle Physics Proceedings, 336–338, 54–61.
11. Zainol, I., Adenan, N., Rahim, N., Jaafar, C. A. (2019). *Extraction of natural hydroxyapatite from tilapia fish scales using alkaline treatment*. Materials Today: Proceedings, 16, 1942–1948.
12. Custodio, C. L., Broñola, P. J. M., Cayabyab, S. R., Lagura, V. U., Celorico, J. R., Basilia, B. A. (2021). *Powder loading effects on the physicochemical and mechanical properties of 3D printed poly lactic Acid/Hydroxyapatite biocomposites*. International Journal of Bioprinting, 7(1), 326.
13. Tazibt, N., Kaci, M., Dehouche, N., Ragoubi, M., Atanase, L. I. (2023). *Effect of filler content on the morphology and physical properties of Poly(Lactic Acid)-Hydroxyapatite composites*. Materials, 16(2), 809.
14. Erokhin, K., Zelinsky, N. D., Ananikov, V. P., Erokhin, K. S., Naumov, S. A. (2023). *Defects in 3D printing and strategies to enhance quality of fff additive manufacturing: A Review*. ChemRxiv, 92(11), available at: https://chemrxiv.org/engage/chemrxiv/article-details/6516b0aba69febde9eea81b1
15. Ndazi, B. S., Karlsson, S. (2011). *Characterization of hydrolytic degradation of polylactic acid/rice hulls composites in water at different temperatures*. Express Polymer Letters, 5(2), 119–131.
16. Zhang, Z., Cao, B., Jiang, N. (2023). *The mechanical properties and degradation behavior of 3d-printed cellulose nanofiber/polylactic acid composites*. Materials, 16(18), 6197, https://doi.org/10.3390/ma16186197
17. Zimina, A., Senatov, F., Choudhary, R., Kolesnikov, E., Anisimova, N., Kiselevskiy, M., Orlova, P., Strukova, N., Generalova, M., Manskikh, V., Gromov, A., Karyagina, A. (2020). *Biocompatibility and physico-chemical properties of highly porous PLA/HA scaffolds for bone reconstruction*. Polymers, 12(12):2938, https://doi.org/10.3390/polym12122938.
18. Dubinenko, G. E., Zinoviev, A. L., Bolbasov, E. N., Novikov, V. T., Tverdokhlebov, S. I. (2020). *Preparation of Poly(L-lactic acid)/Hydroxyapatite composite scaffolds by fused deposit modeling 3D printing*. Materials Today: Proceedings, 22, part 2, 228-234.
19. Ferri, J. M., Jordá, J., Montanes, N., Fenollar, O., Balart, R. (2018). *Manufacturing and characterization of poly(lactic acid) composites with hydroxyapatite*. Journal of Thermoplastic Composite Materials, 31(7), 865–881.
20. Peremel, S., Nor, C., Jaafar, A., Zainol, I., Khairol, M., Ariffin, A. M., Chen, R. S. (2023*). The properties of poly(latic acid) (pla)/hydroxyapatite (fshap) composite prepared through solvent casting techniques*. Malaysian Journal of Microscopy, 19(1), 43–54.
21. Baechle-Clayton, M., Loos, E., Taheri, M., & Taheri, H. (2022). *Failures and flaws in fused deposition modeling (fdm) additively manufactured polymers and composites*. Journal of Composites Science, 6(7), 202.
22. Ko, H. S., Lee, S., Lee, D., & Jho, J. Y. (2021). *Mechanical properties and bioactivity of poly(Lactic acid) composites containing poly(glycolic acid) fiber and hydroxyapatite particles*. Nanomaterials, 11(1), 1–13.

Received: February 25th, 2024 / Accepted: December 15th, 2024 / Paper available online: December 20, 2024